SYMPOSIUM ON SIMULATION IN ARCHITECTURE + URBAN DESIGN
SimAUD 2020

Conditional Generative Adversarial Networks for Pedestrian Wind Flow Approximation

Sarah Mokhtar[1], Aleksandra Sojka[2], and Carlos Cerezo Davila[2]

[1]Kohn Pedersen Fox Associates
London, United Kingdom
smokhtar@kpf.com

[2]Kohn Pedersen Fox Associates
New York, United States of America
{asojka, ccerezodavila}@kpf.com

ABSTRACT

Despite the vital role the wind microclimate plays in urban design, the time, cost and computational expense of wind simulations make them ineffective during early design stages. Surrogate models have been explored as an alternative to the traditional time-consuming computational fluid dynamics (CFD) methods for wind flow approximation in urban contexts. Current approaches, however, have limitations that hinder their applicability and integration in early design pedestrian wind microclimate studies. The high-volume of data generated from CFD simulations provides a practical opportunity for exploring data-driven surrogate models. This paper proposes and evaluates a conditional generative adversarial network surrogate model for the design contribution of urban morphologies to pedestrian wind flow conditions. The validity of the approach is demonstrated at a fraction of the time that would be required to perform the equivalent conventional simulation. Variations in dataset encoding techniques, image resolutions and geometric diversity of the training set are explored to identify the key parameters affecting model's accuracy and suitability for the intended application. Larger urban configuration datasets are recommended to further reduce errors and instill confidence in model predictions for urban contexts quite far from the training set.

Author Keywords

Deep Learning; Performance Simulation; Computational Fluid Dynamics; Generative Adversarial Networks; Surrogate Modeling; Pedestrian Wind Comfort.

1 INTRODUCTION

The ongoing rapid urbanization, with more than 68% of the world's population expected to live in cities by 2050 [1], presents architects, urban designers and city planners with an additional layer of complexity to create livable, resilient and enjoyable cities. In the face of density, cities will face higher vulnerability to climate change, and building professionals will have to design to mitigate the anticipated higher urban heat island effects as well as higher urban wind speeds from high-rise buildings [2]. Wind microclimate studies [3] have extensively explored the relationship between urban morphology and the pedestrian wind conditions, including impacts of building form, building height variations, building arrangements, building porosity, street canyon aspect ratio and orientation. Shaping the built environment to promote favorable wind microclimate conditions can contribute positively to the quality and usability of public spaces through improvements in wind comfort, thermal comfort and air quality through city ventilation and pollution dispersal [2]. These in turn define the activity types and walkability levels which are key to the functioning, vitality and essence of the city.

With design projects increasing in scale from one building to the planning of an entire city, architects and engineers are faced with problems of a complexity that intuition, experience and generic studies insights alone cannot address and where simulation becomes an essential tool to inform design decisions [4]. In response to this growing necessity, several cities have issued and enforced industry standards for the study of a design-contribution to pedestrian wind comfort, including the Dutch NEN 8100 and NPR 6097 in 2006, the EU-RTD COST guidelines in 2007, the Japanese AIJ guidelines in 2008, with the most recent being the wind microclimate guidelines published by the City of London in early 2019. The later recommends the use of either computational fluid dynamics (CFD) or wind tunnel testing or both depending on the complexity of the urban context [5]. Both approaches come with steep time and cost challenges, while CFD has the advantage of providing full flow field data.

Despite the vital role the wind microclimate plays in urban design and its integration in planning regulations, the time, cost and computational expense of wind simulations make them ineffective during early design stages. In practice, the design process is generally characterized by uncertainties in problem definition as well as rapid and frequent changes, both of which necessitate an adaptive, fast, robust [6] and seamlessly integrated simulation workflow [7]. The focus of building performance simulation developments in the past decades, particularly in CFD, has been improving the accuracy rather than speed, a trade-off driven by the low error tolerance in aerospace engineering applications [8]. In contrast to other wind engineering applications, pedestrian wind level (PLW) is "one of the few topics […] where nature is kind to us concerning turbulent flows" [9]. At less constrained comfort ranges and more relaxed error

tolerances, enabling CFD for the exploration and optimization of a large design space through faster methods can provide an understanding of performance variability that bring insights in early design stages that one high-accuracy solution cannot.

In order to address the limited integration of slow feedback conventional CFD simulations in early design optimization workflows [7], a number of approaches have been explored to produce fast approximations models (further expanded in the following section). The high-volume of data generated from CFD simulations provides a practical framework for exploring data-driven surrogate models. End-to-end feature learning through deep learning approaches was shown to be effective in multiple applications in the recent years [10]. This study draws on the opportunity presented to design practitioners to use the CFD simulation data that is produced for multiple projects to train a machine learning model to predict pedestrian urban wind flows during early design explorations. It proposes and evaluates a deep learning methodology, and explores multiple training dataset parameters and encoding strategies as they relate to acceptable error thresholds suitable for the intended application.

2 RELATED WORK

The following review covers different approaches to tackling the high-computational expense of traditional CFD methodologies through both solver approximation and data-driven workflows. It focuses on identifying the approaches' suitability for wind microclimate studies and potential integration in early design architectural and computational process.

2.1 Solver Approximations for CFD

In order to address the time-intensive nature of CFD simulations, a general research focus has been on developing solver approximations. This was achieved through "simplified meshes, use of lower-order equations or the treatment of turbulence through modelling" [8]. For wind microclimate studies, there has been a general focus on the use of steady Reynolds-averaged Navier–Stokes (RANS) simulations. In Toparlar et al.'s review of 183 CFD studies from 1998 to 2015, 96% used RANS despite large eddy simulations (LES)'s potential to provide higher accuracy [3]. At one to two orders of computational time magnitude larger than RANS and a larger modeling complexity [11], the use of LES on practical applications becomes rather limited. This, in turn, reinforces the industry's need for valid but simpler and faster methods for evaluating outdoor urban conditions.

Advanced numerical methods coupled with increased computing capabilities have been investigated to provide from moderate acceleration of conventional approaches to potential real-time CFD feedback. Those can be classified as mesh-based, mesh-free methods and hybrid methods [12]. One approach, which was highly explored in architectural early wind-focused design explorations, is the fast fluid dynamics solver (FFD). Originally developed for real-time fluid visualization in the gaming industry, it gained traction due its notable speed in comparison to RANS [13], about 500-1500 faster on a GPU [14]. In the scope of design exploration, a low Reynolds number model was validated as suitable for simulating air flow inside buildings for natural ventilation applications [15]. It was, however, shown to be less accurate in capturing wind flows between buildings particularly downstream [15], a discrepancy attributed to its lack of turbulence model.

Other GPU-enabled methods are being explored in the context of external urban wind flows. Those include the Smoothed-Particle Hydrodynamics (SPH), a mesh-free approach based on solving particles movement and fluid properties within a certain distance, and the Lattice Boltzman Method (LBM) based on solving the Boltzman equations for particles on a lattice [16]. While those are underway to be developed to suit urban scale applications, they have not yet been demonstrated to provide 'reliable and repeated accuracy' for pedestrian wind comfort applications [16]. Additionally, they rely on high GPU computing requirements and cannot yet be integrated in architectural workflows in a way that can support iterative early design explorations.

2.2 Data-driven CFD approximation models

Machine learning approaches have been proposed as an alternative to approximate wind flow through learning a relationship between geometry represented as input feature vectors and corresponding measured fields [8]. Neural network implementations investigating the urban wind interference impacts are not recent, with early experimentations dating to more than two decades ago [17], [18]. These focused on using wind test data to estimate wind interference factors based on two building separation distances both the along-wind and across-wind directions. More recent studies focused on capturing wind fields from large datasets of full CFD simulations. Artificial neural networks, random forest algorithms and other reduced order models were investigated for approximating wind pressures of buildings with and without urban wind interference impacts [8], [17]–[20]. While effective in relating shape features to interference factors or wind fields, the studies are limited in geometrical parameters and do not provide full field wind flow data for the spaces around buildings. Those limitations, although not directly inferable to urban scale applications, are being challenged in other CFD domains. An example of that is [21] combined a PolyCube novel 3D geometrical representation with a Gaussian method for real-time interactive full field wind speed and pressure for car shape optimization.

2.3 Deep Neural Networks and CFD

The deep neural networks' (DNN) remarkable capability to learn complex, high-dimensional, non-linear dynamic systems, that was shed to light in the last few years, gained

traction in modelling turbulence flows, a high dimensional (spatial and temporal) physical phenomenon [22]. Some of these approaches focused on augmenting physics-based models with their uncertainty quantification and aimed at improving accuracy predictions [23]. Other studies explored applications of DNN models as surrogates for enabling CFD-based design optimization through faster predictions. Deep generative model implementations including convolutional neural networks (CNN) started being particularly explored in this context due to their ability to better represent data in non-linear input and output functions. For instance, Kim et al. [24] constructed, using a CNN, a model that can estimate fluid velocity fields based on data from Eulerian fluid simulations at up to 700 times faster speed than a CPU-CFD. Another example is Guo et al. [10] CNN models that were capable of predicting two and three-dimensional non-laminar flow velocity fields twice as fast as the equivalent GPU-accelerated CFD simulation.

Generative adversarial networks (GAN), which consist of a generator and a discriminator model competing against each other, have been explored as well in predicting fluid behavior due to their additional ability to learn implicit data distributions without the need to define an explicit loss function. An implementation of that is the conditional generative adversarial networks (cGAN) that were used by Farimani et al. [25] for direct predictions of steady state heat conduction and incompressible fluid flow. High accuracy predictions, based entirely on learning from observations, were achieved with a mean absolute error percentage of 1% for different boundary conditions and domains. The deep learning model implementations show the potential of the approach to provide high accuracy inference at state-of-art computational performance in the fluid. Those methodologies can be used to predict steady state flow without any knowledge of fluid flow governing equations and only requiring the encoding of boundary conditions. These results, although promising, are specific to their applications and focused on simple geometries, and thus not generalizable to complex urban systems.

2.4 Limitations and Opportunities

The aspiration for integrating CFD in the early design process has pushed research towards looking into novel methods for fast wind flow approximations. Despite the range of explorations, the current approaches have limitations that prohibit them from being actively used in the urban and architectural design process in the context of pedestrian wind comfort. Advanced numerical methods that are GPU-enabled, such as SPH, LBM and methods, are promising but necessitate high hardware computing requirements, are not integrated in design workflows and have not yet been validated as suitable for predicting external wind flow around buildings. Data-driven workflows, particularly deep learning approaches in CFD, have shown their effectiveness in predicting flow without any knowledge of fluid flow governing equations. The capacity to infer flow fields solely on a set of observations is remarkable and its agnostic nature to the source of the data makes it accessible to a wider audience (architects, engineers, designers …), not limited to any particular software, platform or simulation method and capable of continuously expanding accuracy as more data becomes available. As with the research into accelerated numerical methods, the current workflows tested are specific to the certain applications they were designed for, and results cannot be directly used to infer wind flow in complex urban contexts, neither has their suitability for pedestrian wind comfort applications been explored.

The approach presented in this paper draws on the opportunities that deep learning generative models open for surrogate modeling of physics phenomena and how that can allow for wind-influenced insights into the early design process. The study applies a cGAN to obtain a surrogate model for the design contribution of urban morphologies to pedestrian wind flow conditions. The main contribution of this research is the exploration of the suitability and limitations of this method for the pedestrian wind comfort applications in early design stages, and the evaluation of different training set encoding strategies to identify what simplifications are acceptable for this purpose.

3 METHODOLOGY

The development of a pedestrian wind flow surrogate model for early design stages is proposed based on a cGAN model. This adopted process, represented in Figure 1, starts with the generation of a synthetic dataset based on CFD simulations of procedurally generated urban configurations. An investigation of different geometry representation and dataset encoding techniques are then explored. This is followed by deep learning training, network architecture optimization and finally model evaluation.

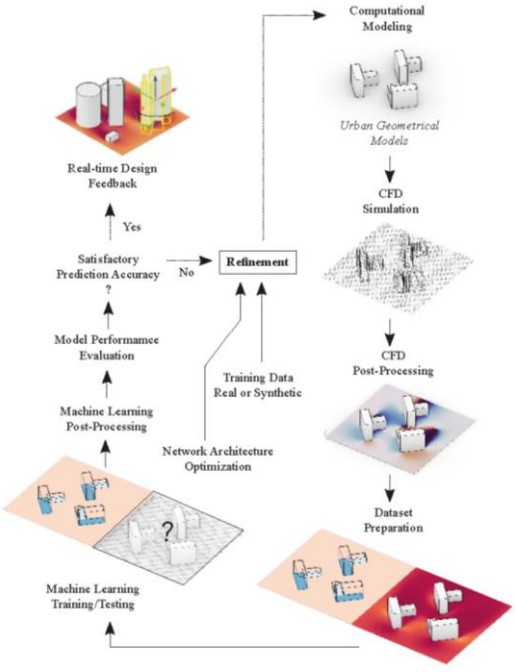

Figure 1. Workflow

A cGAN model architecture for image-to-image translation applications has been adapted for this study based on a PyTorch implementation [26]. This model is an extension to the generative adversarial network (GAN) [27] deep learning model which is composed of two competing networks: a generator, which maps a sample to a desired distribution and a discriminator which determines if a sample belongs to this distribution or has been generated by the generator. The conditional model relies on conditioning an output to an input. In this context, the model inputs and outputs are RGB images with constant pixel count. Abstract and high dimensional data from the geometrical representation of the urban environment is extracted in the encoding layers of the network. These are then mapped, through multiple decoding layers, into wind speed values.

3.1 Urban Geometrical Models

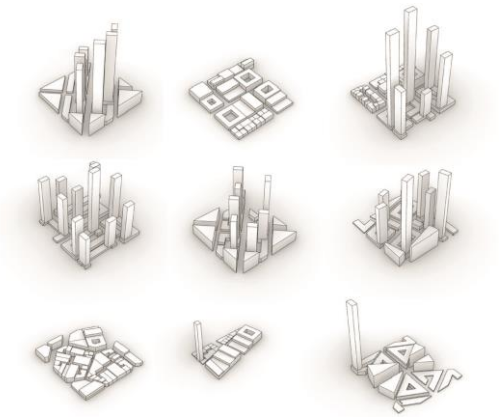

Figure 2. Sample of Urban Geometrical Configurations

Two sets of geometrical configurations were created in order to provide a larger design representation potential: the first set focused on simple configurations of two or three buildings, while the second set provided a larger fidelity to the complexities and rules governing the urban grids and morphologies. These were generated through procedural modelling in Rhinoceros 3D CAD environment using Grasshopper its visual programming environment, while balancing between representability of the urban context and design space dimensionality. The first set included 800 primitive geometries varying in base shape, rotation, relative location within the boundary and height, set within a boundary of 350 m. The second set included 225 urban configurations, varying in grid typology and orientation, density, building morphologies and heights, set within a boundary of 550 m. These were procedurally generated based on typical dimensions and densities of urban contexts.

3.2 CFD Simulation

The *OpenFOAM* solver was used to solve the governing equations of steady-state RANS with a turbulence model of realizable k-ε, following the support in the literature and industry standards for the robustness of this CFD approach for PLW applications [5], [11], [16]. Due to the varying complexity and scales of geometries tested, the time each simulation took to reach convergence ranged from 20 to 120 minutes on a 2.9 GHz i7, running in parallel on Ubuntu Linux distribution. The threshold for convergence was defined as residuals falling below the recommended 10^{-6} [5], which typically meant a termination at around 800 iterations for simple geometries and 2000 for more complex urban configurations. A rectangular domain was used for the analysis, defined as 5 times the maximum building height on the windward, top and sides, and 15 times on the leeward side. The urban configurations tested varied in maximum building height, ranging from 40m to 250m. Cartesian-based 3D structured hexahedral meshing was used at a cell-to-cell expansion ratio of 1.1. A minimum cell size of 3m was selected for this study has been identified as an adequate balance between computational feasibility and a low average error through a sensitivity analysis. A flat terrain was assumed for all cases and a landscape roughness of a dense urban environment was used. At the upstream inlet, a reference wind speed of 6 m/s at a 10m reference height was used for all simulations.

3.3 Geometry Representation and Dataset Preparation

To convert a 3D geometry representation into a 2D matrix, a height map on a Cartesian grid was created for each, where zero level is defined as the wind speed height of interest. In areas where buildings extend beyond the height of interest, a positive distance was assigned, and in other cases, a negative distance to building roofs or ground plane was assigned.

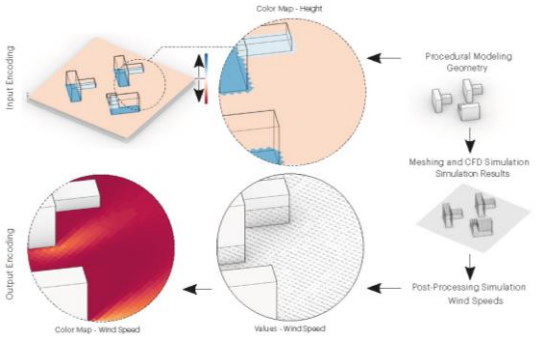

Figure 3. Dataset Encoding

For each simulation case, an automation process was developed through Paraview Python scripting to extract mesh geometries and their corresponding speed values at assigned heights of interest which were selected to range from 1.5m above ground to 36m, at 1.5m intervals. Different data encoding strategies were explored, as listed in Table 1.

Image Sizes	Color Scheme	Colormap Ranges	Training Set Size	Geometric Diversity
256px	Turbo	0 – 8 m/s	5,400	Primitive
512px	Spectral	0 – 16 m/s	13,400	Complex urban
1024px	Inferno	0 – 32 m/s		Hybrid

Table 1. Dataset Encoding and Training Parameters Explored

For the height map matrix and its corresponding speed values, values have been converted to RGB through colormap functions with either 256 or 766 discrete states. To

ensure consistency between input and output images, both were extracted from the same platform. The image pairs were used to create the training and testing sets for the cGAN network. For the first set of urban geometries, 13,800 image pairs were generated, and 5,400 image pairs for the second set of complex urban configurations. For each case, in order to investigate the impacts of image size, colormap functions and colormap ranges on training, multiple sets of each case were created. Three image resolutions were extracted at 256, 512 and 1024 pixels, two high-contrast colormaps were extracted using matplotlib's Spectral and Google AI's Turbo colormap functions and a 766-unique-colors linear colormap function as well in addition to three maximum colormap ranges of 32, 16 and 8 m/s. Image pairs were visually inspected for errors and the dataset was cleared accordingly with a loss of about 15% of the set.

3.4 Network Architecture and Model Training

A Pytorch implementation of a Pix2Pix network architecture [26] was selected. The Pix2Pix model's generator is built with Unet Skip Connection architecture, a variant of encoder-decoder network where the series of convolutional layers of the encoder are 'connected' to deconvolutional layers of the same size of the decoder. The down-sampling (encoder) blocks consist of Convolution-BatchNorm-LeakyReLU layers and the up-sampling (decoder) blocks consist of Deconvolution-BatchNorm-Dropout-ReLU layers. For our experiments, Batch-Normalization was replaced with Instance-Normalization layer for both up-sampling and down-sampling blocks and additional skip connection blocks were added to scale the network up and allow us to train on larger input image sizes, up to 1024x1024 pixels. The model's discriminator follows PatchGAN architecture, a deep convolutional neural network that is designed to classify NxN patches of an input image (generators output) as a real or fake, and then averaging the results, instead of classifying the entire image once. The discriminator model is trained to minimize the negative log likelihood of identifying real and fake images. The generator model is trained using both the adversarial loss for the discriminator model and the L1 loss, the mean absolute difference between the generated translation image and the input image. The generator model had 79.577 M parameters and the discriminator 6.963 M. The datasets were trained for 400 epochs, using kaiming weight initialization, batch size of 32, initial learning rate of 0.0002 with scheduled linear learning rate decay after 200 epochs. After every 5 epochs, the trained weights were saved in order to monitor the progress of the training. Depending on the size of the dataset, the training varied from 500 sec/epoch (4000 x 1024px x 1024px images) to 2500 sec/epoch (12000 x 1024 px x 1024 px images). The training was conducted using several hardware configurations: Windows with two NVIDIA GV100 Volta GPUs with 32MB memory and 128GB RAM; Linux with NVIDIA RTX8000 GPU with 48MB and 128GB RAM; Windows with eight NVIDIA Quadro P6000 GPUs with 24MB memory.

4 RESULTS

To evaluate the accuracy of the proposed framework, the generated wind speed predictions from the cGAN models are compared with the solutions from the RANS CFD simulation. The mean absolute errors (MAE) and 90th percentile errors in m/s are computed for a testing set of 22 geometries unseen to the training network with 528 corresponding image sets. For each image representation, the MAE is defined as the sum of the absolute differences between the predicted and simulated wind speeds for every pixel representation in the image divided by the total number of pixels. Since the interest is in predicting wind flow at pedestrian level, in addition to the cumulative set values, the error was calculated separately for testing image sets below 7.5m height. In addition to a quantitative assessment, a visual inspection of the testing sets further provide an understanding of the models' ability to represent wind behaviors and patterns around buildings and identify zones with highest wind speed amplification.

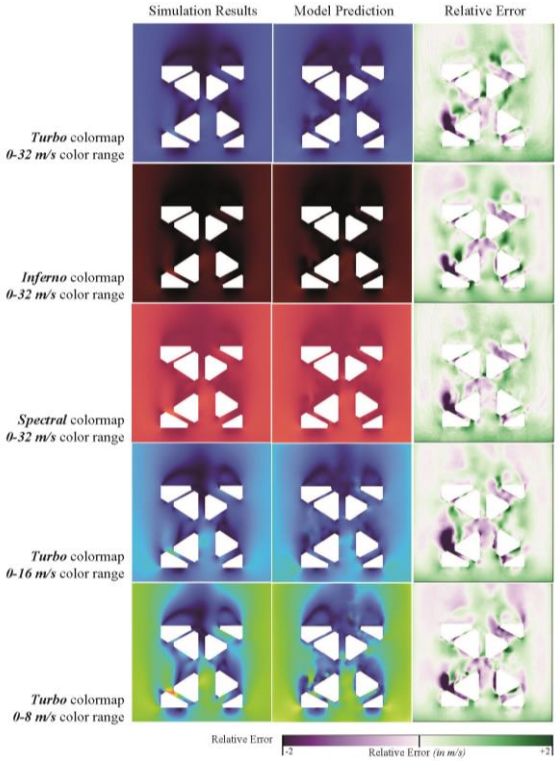

Figure 4. Data Encoding Techniques and Performance

This evaluation method was used to compare different data encoding techniques and training parameters against their corresponding model performance, as illustrated in Figure 4 and 5. Figure 4 illustrates, for the same simulation case, the different data encoding methods used for wind speeds and their respective impact on model prediction errors. The columns from left to right represent the visual representation of simulation results, the corresponding model prediction and the relative error between both. Figure 5 represents a box plot summarizing the MAE and 90th percentile errors for the different encoding strategies and datasets. From left to right,

the represented sets are colormap representations, ranges, building mask color and image size. A distinction is made as well between results of wind speed errors for all trained heights versus pedestrian heights which represent the focus of this work. The selection of data encoding technique for the wind speed was shown to have an impact on the accuracy of the results and can be listed in descending order of impact as: the building mask color, the color range and the color map.

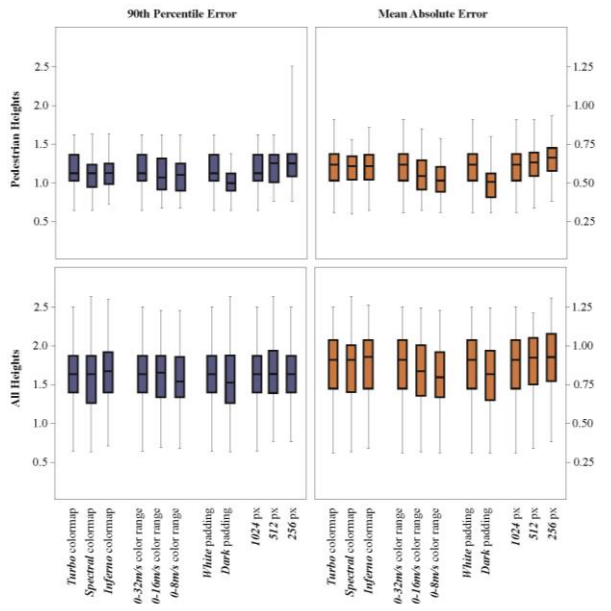

Figure 5. Models' Performance

Firstly, despite being useful for dataset visual inspection, assigning a white color for buildings comes with a disadvantage. A near-grayscale layer of pixels at building edges is observed in many cases and results in the need for a less straightforward building/non-building pixel separation post-process before a conversion to a wind speed matrix is possible. As a by-product, an increase in MAE is observed at an average of 0.1 m/s.

Secondly, a shorter color gradient range representation achieves lower overall MAE of about 0.05 m/s on average as well as more visually legible maps due to the larger number of visually distinct colors. The rare instances in the training set at which high wind speed values reach 16 m/s or more that would be capped by the 0-8 and 0-16 m/s color ranges do not seem to have a significant impact in the overall MAE.

Thirdly, the improvements from the high-contrast smooth visualization of the 'Turbo' and 'Spectral' maps outweighs the three-times larger number of unique colors in the 'Inferno' linear color map. Multiple input training image sizes were as well tested: 1024px, 512px, and 256px. As clear in Figure 4, there is a general improvement observed when training with larger inputs ranging from 0.03 to 0.1 m/s average error difference. This rise in accuracy, however, comes at a steep computational cost, where a 4000-images set training on Windows with 2 GPU/GV100, 32MB memory, 128 GB RAM, would take about 48hrs to complete 400 epochs for a 1024px set compared to 3hrs for 256px. The geometry complexity and diversity of both training and testing sets have the largest noticeable influence on model improvement and prediction accuracies. The first set of training solely included urban geometries with about 4000 training images compared to the same set augmented with simple geometry configurations with about 15000 training images achieved minimally lower accuracy predictions. The larger set, on the other hand, expanded the capacity of the model to infer the morphology contribution to wind speed of both simple building arrangements and dense urban configurations. The predictions accuracy varied as well depending on the deviation of tested instances from the training set geometries. Tested geometries that deviated from the continuous street grids and consistent building morphologies that were generally maintained in the training set corresponded to the highest sources of speed differences.

5 DISCUSSION

Putting the proposed model results in perspective with its intended application to predict pedestrian wind flow conditions around buildings is essential to evaluating its suitability. In contrast to the average MAE of 0.7m/s and the 1.5m/s 90th percentile error for the full testing set, the pedestrian level heights results were capped at an average MAE and 90th error of 0.5m/s and 1.2m/s respectively, decreasing to 0.3m/s and 0.7m/s for urban configurations following the consistent street grids and morphologies it was trained on. Among the comprehensive criteria for pedestrian wind comfort is Lawson criteria which classifies wind speeds in 2m/s interval bands to which is assigned a corresponding percentage of time exceedance. Given the 2m/s-wide band, the proposed model's 0.5m/s MAE reflects its potential suitability for early design pedestrian wind comfort predictions when augmented with a larger repertoire of urban morphologies and further optimizations of the model. The proposed approach presents some challenges and limitations.

Firstly, as with other DNN implementation for physics-informed applications [22], machine learned models are prone to overfitting and there is no direct methodology to ensure that this can be avoided that is applicable to all morphologies that are quite far from the trained dataset, it is essential to cross-validate the model against overfitting. As was observed in the results, although the model was able to infer wind speeds on urban configurations outside the training set, a larger disparity between simulation and model prediction was observed when the continuous street grids and building shapes that the model was trained on was disturbed. This suggests that a larger repertoire of urban morphologies is desirable to further improve its usability, which should be weighed against the computational expense of simulating those with CFD.

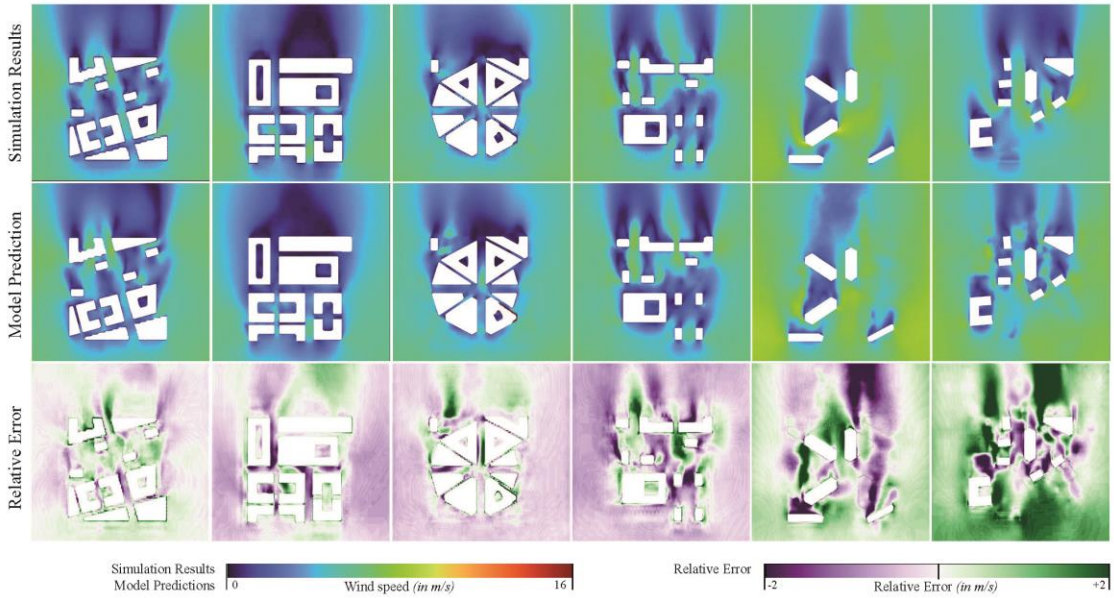

Figure 6. Sample of Model Predictions from Lowest MAE to Highest MAE

Secondly, the current geometry encoding strategy presented can represent a large variety of urban morphologies through an adapted version of a height map. It is, on the other hand, limited to buildings that are continuously solid throughout and cannot yet represent elements such as tunnels, bridges, carved terraces, etc. Other representations of the 3D geometries can be further explored to expand the model capabilities through either augmenting the image encoding for voids using additional color channels or exploring adapted mesh or voxel data structures in a different model architecture.

Thirdly, although applicable to other initial wind speeds, the proposed workflow has only been explored for an initial wind speed at the inlet of 6m/s at a 10m reference height. Different initial wind directions are, on the other hand, possible through rotating the geometry relative to the base south wind direction. In order to overcome the initial wind speed boundary condition limitation, a number of strategies could be further explored. An additional encoding layer to the input representation can be integrated to represent input speed. Another method could be to base the machine learning training on wind factors and use those to infer resulting wind speeds based on the inlet speed.

Fourthly, the lack of structured data for CFD simulations of urban morphologies necessitate the creation of synthetic training sets which require the computationally expensive RANS CFD simulations and thus limit the capability to expand considerably training sets. The challenge here extends beyond solely the computational expense of those simulations, but also the time expense associated with all the automation processes that are needed to convert simulation data into structured datasets suitable for machine learning workflows, as well as the time associated with data and simulation results validation and quality control.

Lastly, as GPU-enabled computational approaches become increasing adopted in the CFD simulation domains and particularly for wind flow in urban contexts, they will present solutions that are significantly more cost effective than CPU-based models. If validated as suitable for pedestrian wind flow studies, they can potentially become viable in the future for faster wind flow approximation, and would substitute the need for data-driven surrogate workflows.

6 CONCLUSION

The paper presented a conditional generative adversarial network approach to developing a surrogate model for the inference of the design contribution of urban morphologies to pedestrian wind flow conditions for any given urban configuration. The developed model is capable of generating pedestrian wind flow approximations for a wide range of urban configurations at an accuracy of about 0.3m/s within seconds, a fraction of what would be needed for a an equivalent CPU-based CFD simulation. For wind microclimate studies, where comfort band ranges are about 2m, the current accuracy results reflect its potential suitability for early design pedestrian wind comfort predictions. The selection of dataset encoding technique, training set parameters and geometrical diversity was shown to have an impact on the accuracy of the results. Those averaged to about 0.1m/s change for each strategy to an accumulated combined 0.3m/s error difference. While some of those improved encoding strategies come with no additional computational cost, the benefit from increased image size and training data size should be evaluated against the corresponding computational expense. The ability of the cGAN to infer wind flow physics from observation was demonstrated and its potential to provide high fidelity results through expanding the training set and further optimizing the

model network was shown to be possible at state-of-the-art computational performance.

ACKNOWLEDGEMENTS

The authors would like to acknowledge the contribution of Theodore Galanos, developer of Butterfly grasshopper plugin, during the workflow development phase, as well to Jason Danforth, colleague at KPF, at the initiation of the research process and initial implementation of the workflow. Thank you to other colleagues at KPF: Max Ogryzko for his initial training experiments and Demi Chang for her work on the parametric urban model.

REFERENCES

[1] United Nations, "World Urbanization Prospects: the 2018 Revision," 2018.

[2] P. Moonen, T. Defraeye, V. Dorer, B. Blocken, and J. Carmeliet, "Urban Physics: Effect of the Micro-climate on Comfort, Health and Energy Demand," *Front. Archit. Res.*, vol. 1, pp. 197–228, 2012.

[3] Y. Toparlar, B. Blocken, B. Maiheu, and G. J. F. van Heijst, "A Review on the CFD Analysis of Urban Microclimate," *Renew. Sustain. Energy Rev.*, vol. 80, pp. 1613–1640, 2017.

[4] S. Hanna, L. Hesselgren, and V. G. Ignacio Vargas, "Beyond Simulation: Designing for Uncertainty and Robust Solutions," in *Proceedings of the 2010 Spring Simulation Multiconference*, 2010.

[5] City of London and RWDI, "Wind Microclimate Guidelines for Developments in the City of London," 2019.

[6] S. Hanna, L. Hesselgren, and V. Gonzalez, "Beyond Simulation: Designing for Uncertainty and Robust Solutions," in *Proceedings of the 2010 Spring Simulation Multiconference*, 2010.

[7] A. Chronis, A. Dubor, E. Cabay, and M. S. Roudsari, "Integration of CFD in Computational Design - An evaluation of the current state of the art," in *Proceedings of the 35th eCAADe Conference*, 2017, pp. 601–610.

[8] S. Wilkinson, G. Bradbury, and S. Hanna, "Reduced-Order Urban Wind Interference."

[9] J. H. Ferziger, "Approaches to Turbulent Flow Computation: Applications to Flow Over Obstacles," *J. Wind Eng. Ind. Aerodyn.*, vol. 35, pp. 1–19, 1990.

[10] X. Guo, W. Li, and F. Iorio, "Convolutional Neural Networks for Steady Flow Approximation | Autodesk Research," in *ACM SIGKDD Conference on Knowledge Discovery and Data Mining*, 2016.

[11] B. Blocken, "LES over RANS in Building Simulation for Outdoor and Indoor Applications: A Foregone Conclusion?," *Build. Simul.*, vol. 11, pp. 821–870, 2018.

[12] M. L. Hosain and R. Bel Fdhila, "Literature Review of Accelerated CFD Simulation Methods towards Online Application," in *Proceesings of the 7th International Conference on Applied Energy (ICAE2015)*, 2015, pp. 3307–3314.

[13] A. Chronis, A. Turner, and M. Tsigkari, "Generative fluid dynamics: integration of fast fluid dynamics and genetic algorithms for wind loading optimization of a free form surface.," 2011, pp. 29–36.

[14] W. Zuo and Q. Chen, "Fast and Informative Flow Simulations in a Building by Using Fast Fluid Dynamics Model on Graphics Processing Unit," *Build. Environ.*, vol. 45, no. 3, pp. 747–757, 2010.

[15] J. Mingang, W. Zuo, and C. Qingyan, "Simulating Natural Ventilation in and around Buildings by Fast Fluid Dynamics," *Numer. Heat Transf. Part A Appl.*, vol. 64, no. 4, pp. 273–289, 2013.

[16] D. Philips and M. Soligo, "Will CFD Ever Replace Wind Tunnels for Building Wind Simulations?," *Int. J. High-Rise Build.*, vol. 8, no. 2, pp. 107–116, 2019.

[17] A. C. Khanduri, C. Bedard, and T. Stathopoulos, "Modelling Wind-Induced Interference Effects using Backpropagation Neural Networks," *J. Wind Eng. Ind. Aerodyn.*, pp. 71–79, 1997.

[18] E. C. English and F. R. Fricke, "The Interference Index and its Prediction using a Neural Network Analysis of Wind-Tunnel Data," *J. Wind Eng. Ind. Aerodyn.*, vol. 83, pp. 567–575, 1999.

[19] S. Wilkinson, S. Hanna, L. Hesselgren, and V. Mueller, "Inductive aerodynamics," 2013.

[20] A. Zhang and L. Zhang, "RBF Neural Networks for the Prediction of Building Interference Effects," *Comput. Struct.*, vol. 83, pp. 2333–2339, 2004.

[21] N. Umetani and B. Bickel, "Learning Three-Dimensional Flow for Interactive Aerodynamic Design," *ACM Trans. Graph.*, vol. 37, pp. 1–10, 2018.

[22] J. Nathan Kutz, "Deep learning in fluid dynamics," 2018.

[23] K. Duraisamy, G. Iaccarino, and H. Xiao, "Turbulence Modeling in the Age of Data," *Annu. Rev. Fluid Mech.*, vol. 51, pp. 357–377, 2019.

[24] B. Kim, V. C. Azevedo, N. Thuerey, T. Kim, M. Gross, and B. Solenthaler, "Deep Fluids: A Generative Network for Parameterized Fluid Simulations," in *Proceedings of EUROGRAPHICS 2019*, 2019, pp. 59–70.

[25] A. B. Farimani, J. Gomes, and V. S. Pande, "Deep Learning the Physics of Transport Phenomena," 2017.

[26] P. Isola, J.-Y. Zhu, T. Zhou, and A. A. Efros, "Image-to-Image Translation with Conditional Adversarial Networks," in *Proceedings of the 2017 IEEE Conference on Computer Vision and Pattern Recognition*, 2017.

[27] I. J. Goodfellow *et al.*, "Generative Adversarial Nets," in *Proceedings of the Advances in Neural Information Processing Systems*, 2014.